arXiv:1405.3594v2 [nucl-th] 26 Aug 2015

Extracting $p\Lambda$ scattering lengths from heavy ion collisions

V.M. Shapoval[a], B. Erazmus[b,c], R. Lednicky[d] and Yu.M. Sinyukov[a]

(*a*) *Bogolyubov Institute for Theoretical Physics,*
Metrolohichna str. 14b, 03680 Kiev, Ukraine

(*b*) *European Organization for Nuclear Research (CERN), Geneva, Switzerland*

(*c*) *SUBATECH, Ecole des Mines de Nantes,*
Université de Nantes, CNRS-IN2P3, Nantes, France

(*d*) *Joint Institute for Nuclear Research, Dubna, 141 980, Russia*

Abstract

The source radii, previously extracted by STAR Collaboration from the $p-\Lambda \oplus \bar{p}-\bar{\Lambda}$ and $\bar{p}-\Lambda \oplus p-\bar{\Lambda}$ correlation functions measured in 10% most central Au+Au collisions at top RHIC energy $\sqrt{s_{NN}} = 200$ GeV, differ by a factor of 2. The probable reason for this is the neglect of residual correlation effect in the STAR analysis. In the present paper we analyze baryon correlation functions within Lednický and Lyuboshitz analytical model, extended to effectively account for the residual correlation contribution. Different analytical approximations for such a contribution are considered. We also use the averaged source radii extracted from the hydrokinetic model (HKM) simulations to fit the experimental data. In contrast to the STAR experimental study, the calculations in HKM show both $p\Lambda$ and $p\bar{\Lambda}$ radii to be quite close, as expected from theoretical considerations. Using the effective Gaussian parametrization of residual correlations we obtain a satisfactory fit to the measured baryon-antibaryon correlation function with the HKM source radius value 3.28 fm. The baryon-antibaryon spin-averaged strong interaction scattering length is also extracted from the fit to the experimental correlation function.

PACS numbers: 13.85.Hd, 25.75.Gz

Keywords: *final state interaction, baryons, scattering length, gold-gold collisions, RHIC, residual correlations*

I. INTRODUCTION

The heavy ion collision experiments provide a good possibility for a study of the baryon-(anti)baryon strong interactions using the Final State Interaction (FSI) correlation technique [1–3]. It is based on the analysis of the momentum correlations caused by final state interactions between corresponding baryons produced in the collision. This activity is especially interesting in view of the ongoing nuclear collision experiments at the LHC, which produce great numbers of various particles, including exotic multi-strange, charmed and beauty ones. It allows one to study the fundamental interactions between specific hadron species, which can hardly be achieved by other means. The extraction of this information makes it possible to check the correctness of hadron-hadron strong interaction models, constrain corresponding interaction potentials, and also improve existing cascade models (like UrQMD) by including into them the information about still unknown baryon-antibaryon annihilation cross-sections.

In the paper [4] the experimental $p\Lambda$ and $p\bar{\Lambda}$ correlation functions measured by STAR at RHIC were fitted with Lednický and Lyuboshitz analytical model [1] allowing, in principle, to extract scattering lengths characterizing the two-particle strong interaction. However, apart from the interaction characteristics, the correlation function depends also on the source spatial structure, described in terms of function $S(\mathbf{r}^*)$, representing the time-integrated separation distribution of particle emission points in the pair rest frame. This fact complicates the study of the particle interaction, as it increases the number of free parameters which enter the fit formula.

To simplify this study, one could calculate the corresponding source functions in realistic models of the collision process, which are known to describe well the experimental observables. The hydrokinetic model [5–7] provides successful simultaneous description of a wide class of bulk observables in the heavy ion collision experiments at RHIC and LHC [8]. Moreover, it reproduces well [9] the pion and kaon source functions for semi-central Au+Au collisions at the top RHIC energy [10], including the specific non-Gaussian tails observed in the pair momentum and beam direction projections of the experimental source function. In

this article we present the results of fitting the experimental data from [4] within the analytical model [1] where the Gaussian parametrization for the emission source function is utilized, and the corresponding Gaussian radii are extracted from the HKM model simulations.

II. MODELS DESCRIPTION

The STAR collaboration studied [4] baryon-baryon $p-\Lambda \oplus \bar{p}-\bar{\Lambda}$ and baryon-antibaryon $p-\bar{\Lambda} \oplus \bar{p}-\Lambda$ correlation functions in 10% most central RHIC Au+Au collisions at $\sqrt{s_{NN}} =$ 200 GeV. Protons and antiprotons in transverse momentum range $0.4 < p_T < 1.1$ GeV/c with the rapidity $|y| < 0.5$, and lambdas and antilambdas with $0.3 < p_T < 2.0$ GeV/c and $|y| < 1.5$ were selected for the analysis.

The experimental correlation function is constructed as the ratio of the distribution of particle momentum in the pair rest frame, k^*, in the same events to the analogous distribution in mixed events. Then the measured correlation function C_{meas} is corrected for the pair purity, defined as the fraction of correctly identified primary particle pairs among all the selected ones, to give the corrected function C_{corr}

$$C_{corr}(k^*) = \frac{C_{meas}(k^*) - 1}{\lambda(k^*)} + 1, \tag{1}$$

where $\lambda(k^*)$ is the pair purity. The estimated mean pair purity in the experiment is $\lambda = 17.5 \pm 2.5\%$.

To fit the experimental correlation function the Lednický and Lyuboshitz analytical model [1] is used, which connects the two-particle correlation function $C(k^*)$ with the particle emission source size r_0 and the s-wave strong interaction scattering amplitudes $f^S(k^*)$ at a given total pair spin S. In the equal-time approximation, valid on condition $|t_1^* - t_2^*| \ll m_{2,1}r^{*2}$ for $\mathrm{sign}(t_1^* - t_2^*) = \pm 1$ respectively, the correlation function can be calculated as a square of the wave function $\Psi^S_{-\mathbf{k}^*}$, representing the stationary solution of the scattering problem with the opposite sign of the vector $\mathbf{k}^*$, averaged over the total spin S and the distribution of the relative distances $S(\mathbf{r}^*)$:

$$C(k^*) = \left\langle \left| \Psi^S_{-\mathbf{k}^*}(\mathbf{r}^*) \right|^2 \right\rangle. \tag{2}$$

In typical nuclear collisions the source radius can be considered much larger than the range of the strong interaction potential, so $\Psi^S_{-\mathbf{k}^*}$ at small k^* can be approximated by the s-wave

solution in the outer region:

$$\Psi^S_{-\mathbf{k}^*}(\mathbf{r}^*) = e^{-i\mathbf{k}^*\cdot\mathbf{r}^*} + \frac{f^S(k^*)}{r^*}e^{ik^*\cdot r^*}. \tag{3}$$

The effective range approximation for the s-wave scattering amplitude is utilized

$$f^S(k^*) = \left(\frac{1}{f^S_0} + \frac{1}{2}d^S_0 k^{*2} - ik^*\right)^{-1}, \tag{4}$$

where f^S_0 is the scattering length and d^S_0 is the effective radius for a given total spin $S = 1$ or $S = 0$.

The particles are assumed to be emitted unpolarized (i.e. with the polarization $P = 0$), so that the fraction of pairs in the singlet state $\rho_0 = 1/4(1 - P^2) = 1/4$, and in the triplet state $\rho_1 = 1/4(3 + P^2) = 3/4$.

The normalized separation distribution (source function) $S(\mathbf{r}^*) = N^{-1}d^3N/d^3\mathbf{r}^*$ is assumed to be Gaussian one

$$S(\mathbf{r}^*) = (2\sqrt{\pi}r_0)^{-3}e^{-\frac{\mathbf{r}^{*2}}{4r^2_0}}, \tag{5}$$

where r_0 is considered as the effective radius of the source.

Under such assumptions the correlation function can be calculated analytically [1]:

$$C(k^*) = 1 + \sum_S \rho_S \left[\frac{1}{2}\left|\frac{f^S(k^*)}{r_0}\right|^2\left(1 - \frac{d^S_0}{2\sqrt{\pi}r_0}\right) + \frac{2\Re f^S(k^*)}{\sqrt{\pi}r_0}F_1(2k^*r_0) - \frac{\Im f^S(k^*)}{r_0}F_2(2k^*r_0)\right], \tag{6}$$

where $F_1(z) = \int_0^z dx e^{x^2-z^2}/z$ and $F_2(z) = (1 - e^{-z^2})/z$. The term $-\frac{d^S_0}{2\sqrt{\pi}r_0}$ in this expression corresponds to the correction accounting for a deviation of $\Psi^S_{-\mathbf{k}^*}$ from the true wave function inside the range of the strong interaction potential. So, the model has quite a large number of parameters, being the scattering lengths f^S_0 and effective radii d^S_0, which may both be complex in general case, and the source radius r_0. Although in principle all of them can be determined from the measured data, in each concrete situation the number of free parameters can be reduced by making certain reasonable assumptions about the values of some of them.

In our study the source radius r_0 is extracted from the Gaussian fit to the source functions calculated in hybrid HKM model. The simulation of the full process of evolution of the system formed in nuclear or particle collision in hybrid HKM consists of two stages. The first one is hydrodynamical expansion of thermally and chemically equilibrated matter described within ideal hydrodynamics approximation with the lattice-QCD inspired equation

of state [11] (corrected for small but nonzero chemical potentials), which is matched with the hadron-resonance gas in chemical equilibrium via cross-over type transition. The second stage consists in gradual system decoupling after loosing chemical and thermal equilibrium. It can be described either within hydrokinetic approach with switching to UrQMD cascade at some space-like hypersurface situated behind the hadronization one, or with sudden switch to UrQMD cascade at the hadronization hypersurface. In current study we choose the second variant of switching to cascade, basing on [8], where the comparison of one- and two-particle spectra, calculated at both types of matching hydro and cascade stages for RHIC and LHC energies, showed a fairly small difference between them.

The model provides particle distribution functions $\frac{d^6N}{d^3xd^3p}$ at the chosen switching hypersurface. Using the Monte-Carlo procedure, one generates particle momenta and coordinates according to these distributions, which serve as the input for the UrQMD hadronic cascade.

To perform a specific calculation one should specify the initial conditions for the hydrodynamics stage attributed to the starting proper time τ_0. These conditions are the initial energy density (or entropy) profile $\epsilon(\mathbf{r})$ and the initial rapidity profile (initial flow) $y(\mathbf{r})$. Here we suppose longitudinal boost-invariance and use $\epsilon(\mathbf{r}_T)$ corresponding to the MC-Glauber model calculated with GLISSANDO code [12]. The maximal energy density ϵ_0 is chosen to reproduce the experimental mean charged particle multiplicity, and the initial flow is supposed to be $y_T = \alpha\frac{r_T}{R^2(\phi)}$, with $\alpha = 0.45$ fm for top RHIC energy. Thus, model has only two free parameters ϵ_0 and α. We start the hydrodynamic evolution at $\tau_0 = 0.1$ fm/c. Sudden switch from hydrodynamics to UrQMD is performed at the isotherm $T = 165$ MeV. The hadron distribution functions (for each hadron sort i) at the switching hypersurface σ_{sw} are calculated according to the Cooper-Frye formula

$$p_0\frac{d^3N_i}{p_T dp_T d\phi_p dy} = \int_{\sigma_{sw}} p^\mu d\sigma_\mu f_i^{eq}(p\cdot u(x), T(x), \mu_i(x)). \tag{7}$$

The procedure of filling the histograms for source functions $S(\mathbf{r}^*)$ (here $\mathbf{r}^*$ is the particle spatial separation in the pair rest frame) can be described by the formula

$$S(\mathbf{r}^{*(k)}) = \frac{\sum_{n=1}^{N_{\rm ev}}\sum_{i_1^n,i_2^n}\prod_{\alpha=1}^{3}[\delta_{\Delta_\alpha}(r_\alpha^{*(k)} - r^*_{i_1^n\alpha} + r^*_{i_2^n\alpha})/\Delta_\alpha]}{\sum_{n=1}^{N_{\rm ev}}\sum_{i_1^n,i_2^n} 1} \tag{8}$$

Here $\mathbf{r}^*_{i_1^n}$ and $\mathbf{r}^*_{i_2^n}$ are the pair rest frame three-coordinates of particles 1 and 2 produced in the $n-$th event, $\mathbf{r}^{*(k)}$ is the three-coordinate of the center of the k-th histogram bin, the

function $\delta_\Delta(x) = 1$ if $|x| < \Delta/2$ and 0 otherwise, and Δ_α is the size of the α-projection of the histogram bin.

III. RESULTS AND DISCUSSION

The $p\Lambda$ source function projections calculated in HKM together with the corresponding Gaussian fits are presented in Fig. 1. Here the out-side-long coordinate system is used, where the *out* axis is directed along the pair total momentum in longitudinally co-moving system, the *long* direction coincides with the beam axis, and the *side* axis is perpendicular to the latter two ones.

One can notice that HKM predicts $p\Lambda$ source function having non-Gaussian tails. The similar behavior was observed experimentally [10] and reproduced in HKM simulations [9] for pion source function. In $p\Lambda$ case these tails appear partially because of the averaging over a wide p_T interval. We also see that in different directions the corresponding Gaussian fits have different widths (especially the *out*-projection is much wider than the other ones). These peculiarities of the HKM separation distribution require, in principle, the generalization of the existing Lednicky-Lyuboshitz formula (6) to the cases of anisotropic non-Gaussian source functions and heavy tails [1]. However, for simplicity and since in the described STAR experiment only one-dimensional correlation function is analyzed with no respect to spatial directions, in current study we are going to stay within the isotropic Gaussian approximation (6) and for this aim utilize the angle-averaged r_0 value. It can be extracted from the Gaussian fit to the angle-averaged source function (see Fig. 2) $S(r) = 1/(4\pi)\int_0^{2\pi}\int_0^{\pi} S(r,\theta,\phi)\sin\theta d\theta d\phi$.

In Figs. 3–6 we present experimental $p-\Lambda \oplus \bar{p}-\bar{\Lambda}$ and $\bar{p}-\Lambda \oplus p-\bar{\Lambda}$ correlation functions, measured by STAR collaboration in 10% most central Au+Au collisions at top RHIC energy $\sqrt{s_{NN}} = 200$ GeV together with the fits performed within Lednický and Lyuboshitz analytical model.

For baryon-baryon case (Fig. 3) the scattering lengths f_0^S and effective radii d_0^S values are taken from [13] ($f_0^s = 2.88$ fm, $f_0^t = 1.66$ fm, $d_0^s = 2.92$ fm, $d_0^t = 3.78$ fm). Thus, the source radius r_0 is the only free parameter in the STAR fit [4] (light curve). Fitting gives $r_0^{exp} = 3.09 \pm 0.30^{+0.17}_{-0.25} \pm 0.2$ fm. In our own fit (dark curve) all the parameters are fixed, and

[1] Note, however, that at such a model extension the number of its free parameters will increase significantly, and utilization of the generalized formula for the reliable description of experimental data will require putting additional constraints on these parameters.

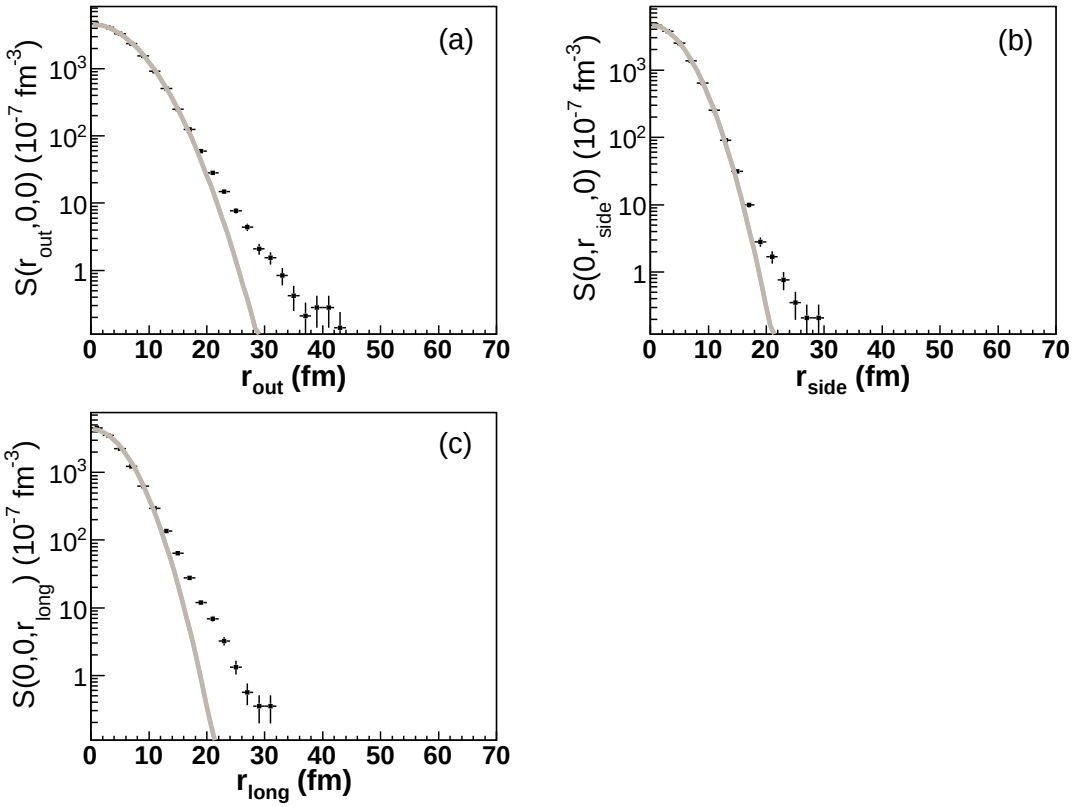

FIG. 1. The $p\Lambda$ source function projections calculated in HKM (markers) and the Gaussian fits to them (lines). The simulations correspond to 10% most central collisions at $\sqrt{s_{NN}} = 200$ GeV in conditions of STAR experiment at RHIC [4]. Pair transverse momentum and rapidity cuts correspond to those in the experiment. The cut $k^* < 50$ MeV/c is also applied to select the pairs from correlation effect domain, where the $r^* - k^*$ correlations are small.

$r_0^{\rm HKM} = 3.23$ fm is determined from a Gaussian fit (5) to calculated in HKM $\mathbf{r}^*$-distribution in the pair rest frame for $r^* < 70$ fm. One can see that HKM model radius is consistent with that extracted from the STAR data in [4].

In the baryon-antibaryon case (Fig. 4) to reduce the number of free parameters both singlet and triplet scattering amplitudes are assumed to be equal, $f^s = f^t = f$ (approximately corresponding to spin-averaged scattering length f_0), and both effective radii are set to zero $d_0^s = d_0^t = 0$ in the STAR fit. The scattering length should have a positive imaginary part $\Im f_0 > 0$ describing the contribution of annihilation channels and leading to a wide dip in the correlation function at intermediate k^*-values due to the last term in Eq. (6). Thus, the model has three free parameters $\Re f_0$, $\Im f_0$ and r_0 in [4] and two free parameters $\Re f_0$, $\Im f_0$ in our fit. The STAR has obtained $p\bar{\Lambda}$ source radius value $r_0 = 1.50 \pm 0.05^{+0.10}_{-0.12} \pm 0.3$ fm

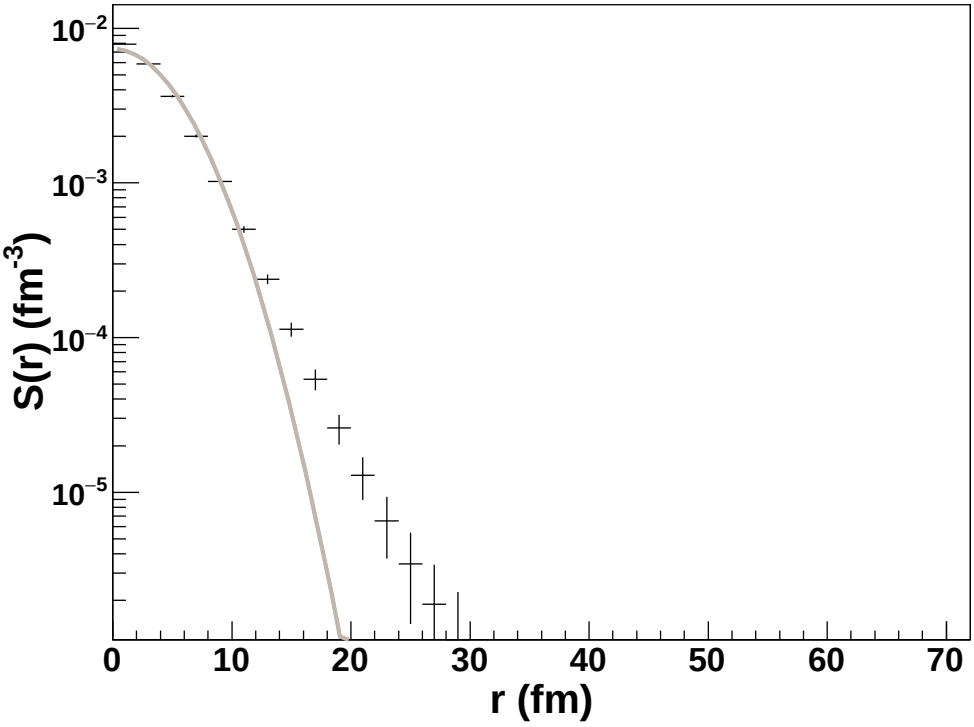

FIG. 2. The $p\Lambda$ angle-averaged source function calculated in HKM (markers) and the Gaussian fit to it (line). The simulation conditions are the same as given in caption of Fig. 1

(light curve), which is ~ 2 times smaller than the $p\Lambda$ one, although there is no apparent physical reason for such a difference. Both radii can be expected to have similar values, and the HKM source radius for the baryon-antibaryon case $r_0^{\rm HKM} = 3.28$ fm is expectedly close to the corresponding baryon-baryon one. But at this source radius the fitting curve (dark) is too narrow to describe the data points.

However, residual correlations were not taken into account in the STAR analysis [4, 14]. Constructing the experimental correlation function one usually supposes that only the pairs composed of two primary particles are correlated, and the rest of the pairs, which include secondary or misidentified particles, are supposed to be uncorrelated. However, among such pairs the so-called residual correlations can exist. They occur if the parent of a particle from such a pair was correlated with another particle forming the pair. For example, if Σ^+, correlated with some Λ, decays into proton and π^0, then this proton will be residually correlated with the Λ. The interactions in most of such pairs are unknown, so at the moment there is no possibility to reliably refine the constructed experimental correlation function from the effect of residual correlations. However, one can try to account for the residual correlations at least phenomenologically using a simple analytical approximation to

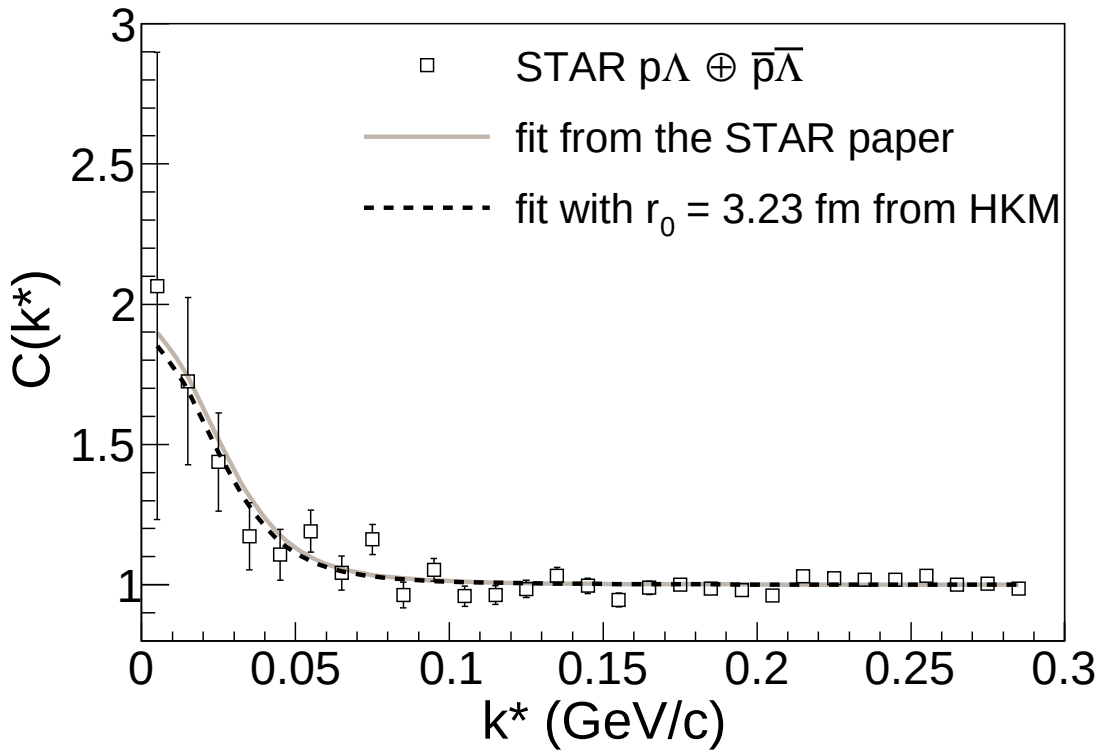

FIG. 3. The $p-\Lambda\oplus\bar{p}-\bar{\Lambda}$ correlation function measured by STAR (open markers), the corresponding fit according to (6) with parameters fixed as in the STAR paper [4] within the Lednický and Lyuboshitz analytical model [1] (light solid line) and our fit within the same model with the source radius r_0 extracted from the HKM calculations (dark dashed line).

the residual correlation function.

Note that the effect of the residual correlations has presumably only a minor influence on the baryon-baryon $p\Lambda$ correlation function since in this case there are not so many inelastic channels open for parent FSI near threshold and if open, they are usually suppressed also being near threshold. So, $\Im f_0$ for parent pairs (giving negative contribution to residual correlation function) is expected to be small and the sign of $\Re f_0$ may vary from one parent pair to another, thus likely reducing the net effect of $\Re f_0$ on residual correlation function.

In contrast to this, in case of $\bar{p}\Lambda$ correlation function there is a number of annihilation channels significantly contributing to $\Im f_0$ and leading to a substantial negative contribution to residual correlation function.

In the case when the measured baryon-antibaryon correlation function is not corrected for purity, the fitted uncorrected correlation function is expressed through the true one in

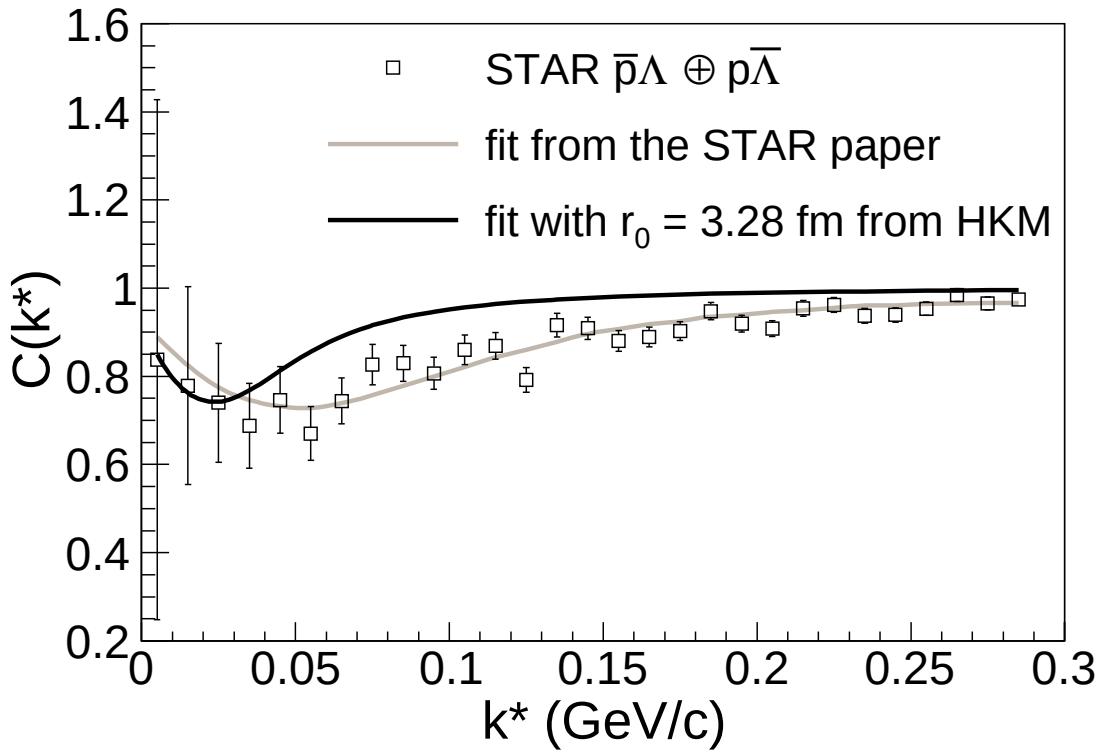

FIG. 4. The same as in Fig. 3 for the $\bar{p} - \Lambda \oplus p - \bar{\Lambda}$ correlation function.

(6) similar to (1):

$$C_{uncorr}(k^*) = \lambda(k^*)C(k^*) + (1 - \lambda(k^*)), \tag{9}$$

The pair purity $\lambda(k^*)$ in our calculations is extracted according to (9) from the plots of $C_{\rm uncorr}(k^*)$ and $C(k^*)$ provided in [16].

The first term in formula (9) corresponds to the pairs of correlated (primary only) particles, and the second one represents the contribution of the uncorrelated pairs, where one or both particles are misidentified or secondary ones. Assuming that among the latter there can be residually correlated pairs, one should modify this expression to account for the residual correlations as well.

In the recent paper [14], the account for residual correlations is performed by summarizing all the contributions from different parent pairs to the full correlation function, making, however, a number of simplifying assumptions. Particularly, the purity k^*-dependence is neglected in their analysis. As for the scattering parameters f_{0i} and d_{0i} of the parent systems and the corresponding parent source radii r_{0i}, the effective range parameters d_{0i} are neglected and f_{0i} and r_{0i} are assumed to be equal to universal baryon-antibaryon values.

As compared with [14], we propose here the alternative approach avoiding such a detailed (containing however a number of assumptions) calculation of the residual correlations. Instead, we are aiming to describe them by introducing some effective residual correlation function $C_{\rm res}(k^*)$ for a fraction $\alpha(k^*)$ of the pairs of particles supposed earlier in Eq. (9) uncorrelated. Then,

$$C_{uncorr}(k^*) = 1 + \lambda(k^*)(C(k^*) - 1) + \alpha(k^*)(C_{res}(k^*) - 1). \tag{10}$$

Obviously, Eq. (10) reduces to Eq. (9) if either $C_{\rm res}(k^*) = 1$ or $\alpha(k^*) = 0$. One may approximate $\alpha(k^*)$ with a constant (e.g., put $\alpha = 0.49$, which is the total fraction of the pairs containing daughter particles as given in table III of [4]) or assume it proportional to the fraction of non-primary particles: $\alpha(k^*) = \tilde{\alpha}[1 - \lambda(k^*)]$, where $\tilde{\alpha}$ is a fit parameter.

Choosing the concrete form of $C_{\rm res}(k^*)$ requires some additional analysis. First of all, one should take into account that due to the phase space suppression of small k^*-values, the baryon-antibaryon correlations are dominated by the effect of wide annihilation dips in parent correlation functions related with $\Im f_{0i}$ through the negative last term in Eq. (6). The parent decays widen these dips and wash out possible structures at small k^* related with $\Re f_{0i}$. Further, the contribution to the $C_{\rm res}(k^*)$ from a given parent correlation function recovers the latter for k^* larger than the parent decay momenta, i.e. for sufficiently large $z = 2k^* r_0$ [15]. Moreover, following from large-z behavior of the functions $F_1(z) \to (2z)^{-2}$ and $F_2(z) \to z^{-1}$, the parent correlation functions approach unity from below according to a universal inverse power law $\propto z^{-n}$, where the power $n > 2$ increases with the number of terms essentially contributing in the effective range expansion in a given k^*-interval. Particularly, $n = 3$ if one may neglect already the effective range parameters d_{0i} (i.e. neglect the k^*-dependence of the effective range function):

$$C_i(z) - 1 \to \frac{-u + v/(\sqrt{\pi} z)}{z[(1 + uz/2)^2 + (vz/2)^2]} \to z^{-3}, \tag{11}$$

where $u = \Im f_{0i}/r_{0i}$, $v = \Re f_{0i}/r_{0i}$. For practical calculations, one may follow [14] and assume approximately the same source radii and scattering parameters for all baryon-antibaryon systems. Then, one can approximate $C_{\rm res}(z)$ at large enough z by the $\bar{p}\Lambda$ correlation function $C(z)$ and approximately account for the washing out effect of parent decays by smoothly tailing the latter at some value $z = z_t$ to a slowly varying function $1 - A + Bz^c$:

$$C_{res}(z, z \le z_t) = 1 - A + Bz^c,$$

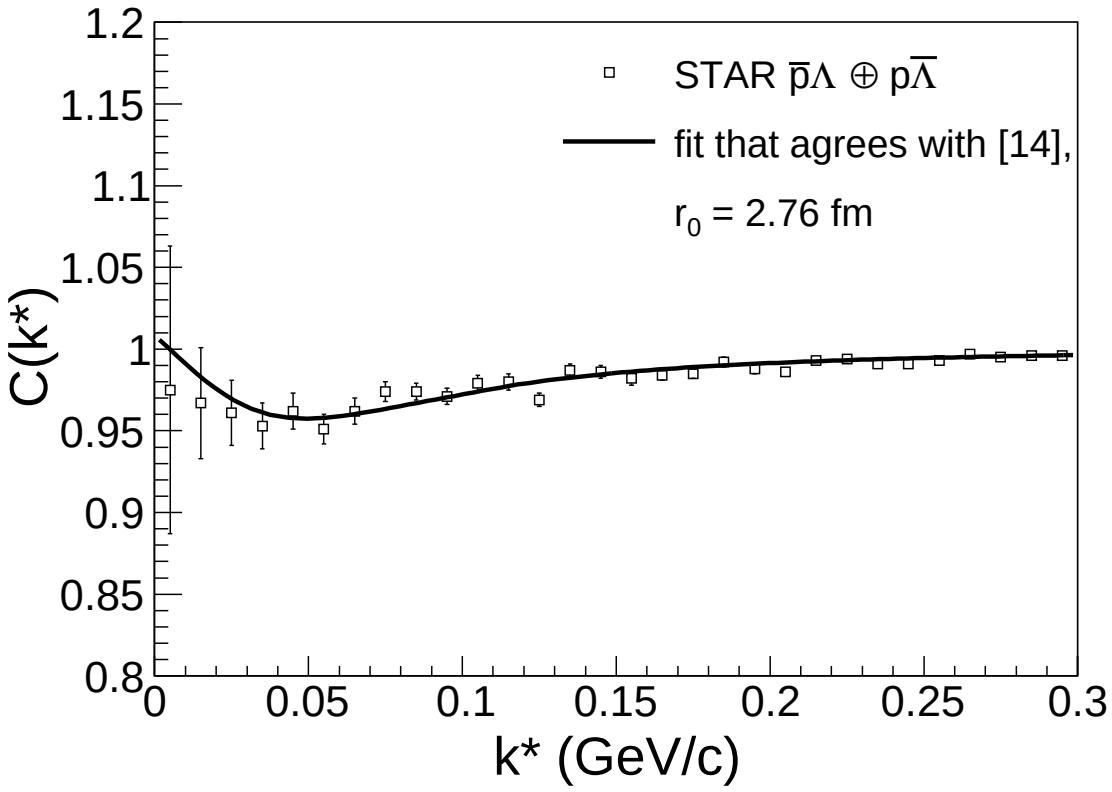

FIG. 5. Our fit (black line) to the STAR purity uncorrected $\bar{p}-\Lambda \oplus p-\bar{\Lambda}$ correlation function as presented in [14] (open markers) according to (10), (6), with $C_{res}(k^*)$ term in the form (12). In this particular fitting the source radius r_0 is a free parameter. The extracted fit parameter values are $r_0 = 2.76 \pm 0.13$ fm, $\Re f_0 = 0.59 \pm 0.19$ fm, $\Im f_0 = 0.85 \pm 0.14$ fm, with $\chi^2/\mathrm{ndf} = 1.37$.

$$C_{res}(z, z > z_t) = C(z). \tag{12}$$

Using the effective expression (12) for C_{res} and data points from [14], one can reproduce the results obtained in [14] but in much simpler way. So, assuming $\alpha(k^*) = 0.49$ and $\lambda(k^*) = 0.15$ as in [14] and fixing $z_t = 3$, $c = 1.5$ based on the analysis of various contributions to the residual correlation function including those in Fig. 4 in [14], the fit results are: $r_0 = 2.76 \pm 0.13$ fm, $\Re f_0 = 0.59 \pm 0.19$ fm, $\Im f_0 = 0.85 \pm 0.14$ fm, with $\chi^2/\mathrm{ndf} = 1.37$ (see Fig. 5). They agree within the errors with the result from [14]: $r_0 = 2.83 \pm 0.12$ fm, $\Re f_0 = 0.49 \pm 0.21$ fm, $\Im f_0 = 1.00 \pm 0.21$ fm. The fitted r_0 value agrees with the fit result for $p\Lambda$ system, however, it is substantially smaller than the HKM prediction of 3.28 fm. As a result, the fit with the radius fixed at the HKM value leads to unsatisfactory description of the correlation function.

Therefore, sticking on the HKM result, one is enforced to apply a more flexible parametrization of $C_{\rm res}$, avoiding the assumption of the universal form of baryon-antibaryon correlation functions at $z > z_t$ with a constant effective range function (i. e. with neglected d_0 and higher order expansion parameters). It is worth noting that even if keeping the universality assumption, the account of additional complex expansion parameters would make the fit quite unstable and unpractical at given statistical errors. Instead, one can use the effective Gaussian parametrization with reasonable behavior at small and large k^*-values [17, 18]:

$$C_{res}(k^*) = 1 - \tilde{\beta} e^{-4k^{*2}R^2}, \tag{13}$$

where $\tilde{\beta} = A > 0$ is the annihilation (wide) dip amplitude and $R \ll r_0$ is the dip inverse width.

Choosing further the fraction of residually correlated particles as $\alpha(k^*) = \tilde{\alpha}[1 - \lambda(k^*)]$, one may notice that the parameters $\tilde{\alpha}$ and $\tilde{\beta}$ enter in (10) only through a product $\tilde{\alpha}\tilde{\beta}$, the latter can be substituted by a single fit parameter β.

In Fig. 6 we present the result of such a fit of the experimental $\bar{p}\Lambda \oplus p\bar{\Lambda}$ correlation function. The fit quality is quite good ($\chi^2/\mathrm{ndf} = 0.87$) and the fitted parameters are: $\Re f_0 = 0.14 \pm 0.66$ fm, $\Im f_0 = 1.53 \pm 1.31$ fm, $\beta = 0.034 \pm 0.005$ and $R = 0.48 \pm 0.05$ fm. Unfortunately, due to the decoupling of the form of the residual correlation function from the scattering parameters, the statistics now apperars to be insufficient for their reliable determination.

IV. CONCLUSIONS

Study of baryon and antibaryon correlations provides a powerful tool for probing space-time evolution of heavy ion collisions and for extracting the parameters of strong interaction between emitted particles.

We reproduced the $p-\Lambda \oplus \bar{p}-\bar{\Lambda}$ and $\bar{p}-\Lambda \oplus p-\bar{\Lambda}$ correlation functions, measured in 10% most central Au+Au collisions by STAR at $\sqrt{s_{NN}} = 200$ GeV, using Lednicky and Lyuboshitz analytical formalism with the average source radii extracted from the hydrokinetic model (HKM). To take into account the residual correlations influencing baryon-antibaryon femtoscopic effects, a modified analytical approximation has been applied. The values of the $p\Lambda$ and $p\bar{\Lambda}$ source radii calculated in HKM are similar, in agreement with theoretical

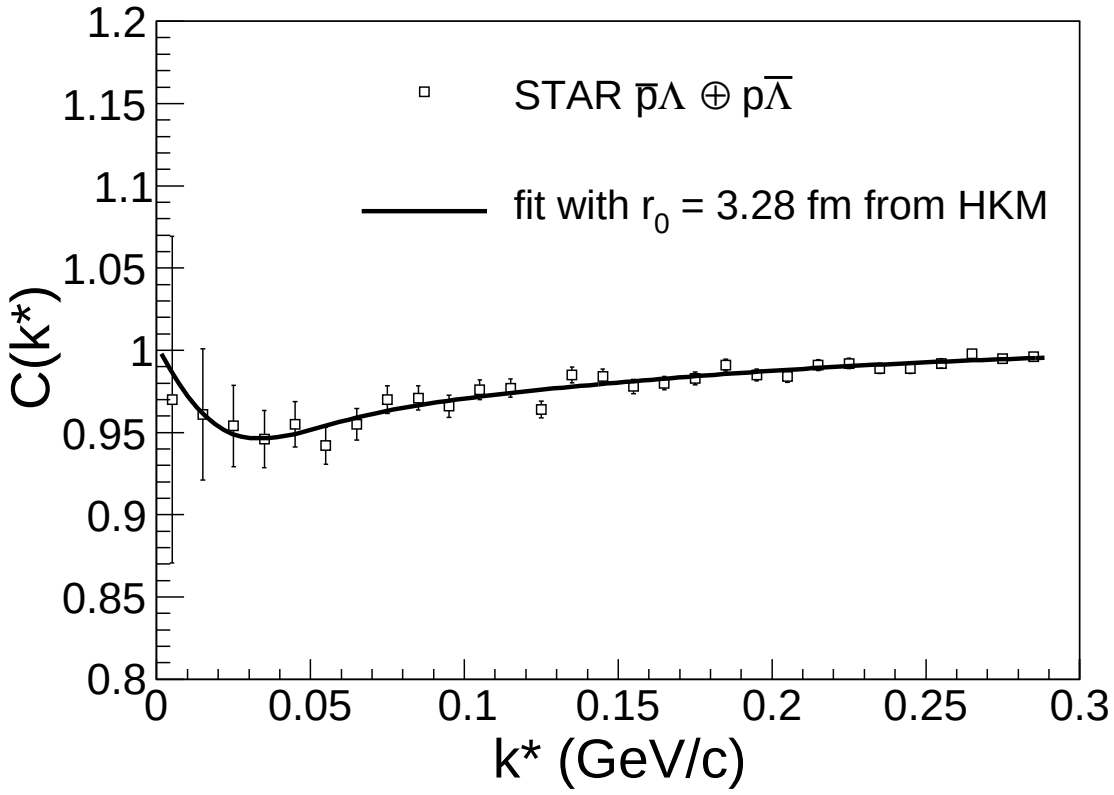

FIG. 6. The purity uncorrected $\bar{p} - \Lambda \oplus p - \bar{\Lambda}$ correlation function measured by STAR [16] (open markers) and our fit to it according to (10) and (6) (black line), with the Gaussian parametrization (13) for the residual correlation term $C_{res}(k^*)$. The source radius r_0 was fixed at a value extracted from the HKM calculations. The extracted fit parameters are $\Re f_0 = 0.14 \pm 0.66$ fm, $\Im f_0 = 1.53 \pm 1.31$ fm, $\beta = 0.034 \pm 0.005$ and $R = 0.48 \pm 0.05$ fm, with $\chi^2/\mathrm{ndf} = 0.87$.

expectations, and consistent with experimental result for $p - \Lambda \oplus \bar{p} - \bar{\Lambda}$. The significantly smaller source size obtained by the STAR Collaboration for $\bar{p} - \Lambda \oplus p - \bar{\Lambda}$ pairs can be explained by neglecting residual correlations at the data analysis.

The real and imaginary parts of the spin averaged scattering lenghts have been extracted for baryon-antibaryon pairs when residual correlations are taken into account. We analyse the different forms of effective corrections for the residual baryon-antibaryon correlations, and find that the simple Gaussian form results in the best fit quality.

The hydrokinetic model including a detailed description of particle correlations allows for a precise study of heavy ion collisions. New high statistics data from RHIC and LHC will provide measurements of various particle pairs, including baryon-antibaryon ones, allowing

to investigate the particle interactions in these pairs. A consistent approach for a wide class of observables will help to understand complex and unknown features of the evolution of heavy ion collisions.

V. ACKNOWLEDGMENTS

The authors are grateful to Iurii Karpenko for his assistance with computer code. The research was carried out within the scope of the EUREA: European Ultra Relativistic Energies Agreement (European Research Group: "Heavy ions at ultrarelativistic energies") and is supported by the National Academy of Sciences of Ukraine (Agreements F6-2015 and MVC1-2015).

[1] R. Lednický, V. L. Lyuboshitz, Yad. Fiz. **35**, 1316 (1981) [Sov. J. Nucl. Phys. **35**, 770 (1982)]; in Proceedings of the International Workshop on Particle Correlations and Interferometry in Nuclear Collisions (CORINNE 90), Nantes, France, 1990, edited by D. Ardouin (World Scientific, Singapore, 1990), pp. 4254; R. Lednicky, J. Phys. G: Nucl. Part. Phys. **35** (2008) 125109.

[2] L. Nemenov, Yad. Fiz. **41**, 980 (1985); V.L. Lyuboshitz, Yad. Fiz. **48**, 1501 (1988) [Sov. J. Nucl. Phys. **48**, 956 (1988)].

[3] Yu.M. Sinyukov, R. Lednický, S.V. Akkelin, J. Pluta, and B. Erazmus, Phys. Lett. B **432**, 248 (1998).

[4] J. Adams *et. al.* (STAR), Phys. Rev. C, **74**, 064906 (2006).

[5] Yu.M. Sinyukov, S.V. Akkelin, and Y. Hama, Phys. Rev. Lett. **89**, 052301 (2002).

[6] S.V. Akkelin, Y. Hama, Iu.A. Karpenko, Yu.M. Sinyukov. Phys. Rev. C **78**, 034906, (2008).

[7] Iu.A. Karpenko, Yu.M. Sinyukov. Phys. Rev. C **81** 054903, (2010).

[8] Iu.A. Karpenko, Yu.M. Sinyukov, K. Werner. Phys. Rev. C **87**, 024914, (2013).

[9] V.M. Shapoval, Yu.M. Sinyukov, and Iu.A. Karpenko, Phys. Rev. C **88**, 064904, (2013).

[10] S. Afanasiev *et al.* (PHENIX Collaboration), Phys. Rev. Lett. **100**, 232301 (2008).

[11] M. Laine, Y. Schröder, Phys. Rev. D **73**, 085009 (2006).

[12] W. Broniowski, M. Rybczynski, P. Bozek, Comput. Phys. Commun. **180**, 69 (2009).

[13] F. Wang and S. Pratt, Phys. Rev. Lett. 83, 3138 (1999).

[14] A. Kisiel, H. Zbroszczyk and M. Szymanski, Phys. Rev. C **89**, 054916 (2014), arXiv:1403.0433.

[15] A. Stavinskiy, K. Mikhailov, B. Erazmus, R. Lednicky, arXiv:0704.3290.

[16] G. Renault for the STAR Collaboration, Acta Phys. Hung. A**24**, 131 (2005).

[17] V. M. Shapoval, B. Erazmus, R. Lednicky, Yu. M. Sinyukov, arXiv:1405.3594v1 [nucl-th]

[18] L. Adamczyk *et. al.* (STAR), arXiv:1408.4360[nucl-ex].